

Original Article

Human umbilical cord mesenchymal stem cells enhance liver regeneration and decrease collagen content in fibrosis mice after partial hepatectomy by activating Wnt/ β -catenin signaling

Xuewei Li^{1,†}, Jinghui Feng^{2,†}, Haiqin Cheng¹, Ning Jin¹, Shanshan Jin¹, Zhizhen Liu¹, Jun Xu³, and Jun Xie^{1,*}

¹Department of Biochemistry and Molecular Biology, Shanxi Key Laboratory of Birth Defect and Cell Regeneration, MOE Key Laboratory of Coal Environmental Pathogenicity and Prevention, Shanxi Medical University, Taiyuan 030001, China, ²Academy of Medical Sciences, Shanxi Medical University, Taiyuan 030001, China, and ³Department of Hepatobiliary and Pancreatic Surgery and Liver Transplant Center, the First Hospital of Shanxi Medical University, Taiyuan 030001, China

Received 28 April 2024 Accepted 17 July 2024 Published 23 December 2024

Abstract

Liver fibrosis is a critical stage in the progression of various chronic liver diseases to cirrhosis and liver cancer. Early inhibition of liver fibrosis is crucial for the treatment of liver disease. Hepatectomy, a common treatment for liver-related diseases, promotes liver regeneration. However, in the context of liver fibrosis, liver regeneration is hindered. Many studies have shown that mesenchymal stem cells (MSCs) can promote liver regeneration after partial hepatectomy (PH). However, there are few reports on the impact of MSC therapy on liver regeneration post-PH in the context of hepatic fibrosis. The objective of this study is to examine the impact of MSCs on liver regeneration following PH in the fibrotic liver and uncover the related molecular mechanisms. This study reveals that MSC therapy significantly enhances liver function and mitigates liver inflammation after PH in the context of hepatic fibrosis. MSCs also significantly promote liver regeneration and alleviate liver fibrosis. In addition, this study identifies the role of MSCs in promoting liver regeneration and alleviating liver fibrosis via the activation of Wnt/ β -catenin signaling. The combination of MSCs with hepatectomy may offer a novel approach for the treatment of liver fibrotic diseases.

Key words liver fibrosis, liver regeneration, partial hepatectomy, mesenchymal stem cells

Introduction

As the largest and most important metabolic organ, the liver is crucial for substance synthesis and decomposition, energy metabolism, immune response, and detoxification. However, long-term chronic viral infection, alcohol, obesity, drugs, and toxins can cause irreversible liver damage. Chronic liver injury often leads to liver inflammation, fibrosis, cirrhosis, and even liver cancer [1]. Globally, approximately 1 to 1.2 million people die annually from liver fibrosis, cirrhosis, liver cancer, or their complications, significantly reducing life expectancy [2].

Liver fibrosis is characterized by excessive accumulation of

extracellular matrix [3], and chronic liver injury poses a significant global health concern [4]. Hepatic stellate cells (HSCs) are crucial in the development and progression of hepatic fibrosis [5]. Unfortunately, effective treatments for liver fibrosis are limited to addressing the underlying cause or opting for liver transplantation [6].

One of its most remarkable features is the ability of the liver to regenerate from damage. In healthy individuals, the liver can compensate for the acute loss of up to 70%–75% of its total mass [7–9]. This regenerative ability makes living donor liver transplantation and partial hepatectomy (PH) possible [10,11]. Both procedures necessitate swift liver regeneration to maintain proper

[†]These authors contributed equally to this work.

^{*}Correspondence address. Tel: +86-351-3985008; E-mail: junxie@sxmu.edu.cn

liver function and overall homeostasis.

Most patients who undergo hepatectomy also suffer from liver fibrosis. In China, over 80% of liver cancer patients have underlying liver conditions such as fibrosis or cirrhosis, often necessitating partial hepatectomy. Promoting the recovery of liver function after PH remains a significant surgical challenge.

Mesenchymal stem cells (MSCs) contribute to immune regulation, tissue repair and angiogenesis. Owing to their potential for multidirectional differentiation, MSCs have garnered significant attention and have been applied in the clinical treatment of various chronic diseases, becoming a cornerstone of cell therapy. Numerous studies have confirmed that MSC therapy can enhance liver regeneration after liver PH [12–15]. However, the effect of MSC therapy on liver regeneration in models with impaired liver regeneration, such as liver fibrosis and cirrhosis, remains unexplored.

Recent research has examined the potential of MSCs to alleviate liver fibrosis and enhance liver function [16–18]. MSCs of various origins have demonstrated antifibrotic potential in animal models [19–21]. The possible mechanisms include the ability of MSCs to replace damaged hepatocytes, promote hepatocyte regeneration, and inhibit or induce apoptosis in HSCs, thereby reducing liver fibrosis [22].

Previous studies have shown that Wnt/ β -catenin signaling is pivotal in embryonic development and tumor progression [23,24]. This pathway also plays a significant role in liver development, maturation, and differentiation [24,25]. In a mature and healthy liver, Wnt/ β -catenin signaling is mostly inactive. However, during cell renewal or regeneration and in pathological conditions such as disease, inflammation, or malignant tumors, this pathway is reactivated and becomes important for liver regeneration and repair.

The purpose of this study was to examine changes in the regenerative ability of liver fibrosis after PH compared with that of normal liver tissue; to assess improvements in fibrosis in the regenerated liver; and to explore the therapeutic effects, mechanisms, and influence of human umbilical cord-derived mesenchymal stem cells (H-uc MSCs) on liver regeneration after PH in liver fibrosis. Additionally, this study analyzes the function of Wnt/ β -catenin signaling in liver regeneration after liver PH in hepatic fibrosis. Our results demonstrate for the first time that MSCs significantly promote liver regeneration after liver PH and effectively reduce liver fibrosis via Wnt/ β -catenin signaling, suggesting that H-uc MSCs constitute a novel approach for treating liver fibrotic diseases.

Materials and Methods

Extraction and identification of H-uc MSCs

Fresh umbilical cord specimens were obtained from pregnant women undergoing cesarean section, with informed consent signed before specimen acquisition. MSCs were isolated and cultured following the method described by Fu *et al.* [26]. The cells were cultured in DMEM-F12 (Gibco, New York, USA) enriched with 10% FBS (Gibco) and 1% antibiotics at 37°C in a humidified atmosphere with 5% CO₂. The morphology of H-uc MSCs was observed via phase-contrast microscopy (Eclipse TE200; Nikon, Tokyo, Japan). Cells from the fifth passage were utilized in this study.

When the cells reached 70% to 80% confluence, the medium was replaced by osteogenic differentiation medium (A1007201; Gibco)

and adipogenic differentiation medium (A1007001; Gibco). After approximately 14 days, Oil Red O staining and Alizarin Red S staining were performed to identify osteoblasts and adipocytes, which were then observed and photographed under an optical microscope. MSC phenotypes were identified via a Human MSC Analysis Kit (562245; BD, Franklin Lakes, USA) via FACS Celesta flow cytometry. According to the kit instructions, MSCs should be positive for CD73, CD90, and CD105 but negative for markers included in PE (CD34, CD11b, CD19, CD45, and HLA-DR).

Animal models and experimental design

C57BL/6 male mice (Vital River Laboratory Animal Technology, Beijing, China), aged 6-8 weeks, were selected for the study. The mice were kept in a standard animal laboratory environment with a regular diet and light cycle. Following several days of acclimatization, the mice were randomly allocated into four groups (n = 6 per group): the control group, Oil + PH group, CCl₄ + PH group and CCl₄ + PH + MSC group. A 70% hepatectomy involving ligation and resection of the left and middle lobes of the liver was performed according to previously described methods [27]. The control group and the Oil + PH group received intraperitoneal injections of olive oil (Aladdin, Shanghai, China; 1.5 ml/kg, once every 3 days, for 9 weeks). The other two groups were prepared with CCl₄ (Damao Chemical Reagent Factory, Tianjin, China) and olive oil (1:3 volume ratio) at the same dosage and schedule [28,29]. After 9 weeks, the control group underwent laparotomy to free the falciform ligament of the liver. The abdomen was subsequently closed without further treatment. The other 3 groups were subjected to 70% PH [27,30,31]. The CCl₄ + PH + MSC group was injected with H-uc MSCs (1 x 10⁶ cells/piece) through the tail vein before abdominal closure. The CCl₄ + PH group received an equivalent volume of normal saline.

On day 7, the mice were sacrificed, and liver and serum samples were collected. A portion of the liver tissue was fixed in 4% paraformaldehyde, embedded in paraffin, and sectioned. The remaining liver tissue was frozen in liquid nitrogen and stored at -80°C for subsequent experiments. All the experimental procedures and methods are shown in Figure 1A.

Biochemical analysis

Blood samples were centrifuged at 4° C and 1500 g for 15 min to obtain serum. The alanine aminotransferase (ALT) and aspartate aminotransferase (AST) levels were determined with an alanine aminotransferase assay kit (C009-2-1; Nanjing Jiancheng Biotechnology, Nanjing, China) and an aspartate aminotransferase assay kit (C010-2-1; Nanjing Jiancheng Biotechnology), respectively. The alkaline phosphatase (ALP) and γ -glutamyl transferase (γ -GT) levels were measured via an alkaline phosphatase assay kit (A059-2-1; Nanjing Jiancheng Biotechnology) and a γ -glutamyl transferase assay kit (C017-2-1; Nanjing Jiancheng Biotechnology). To determine the collagen level in liver tissue, hydroxyproline (Hyp) level was assessed via a hydroxyproline assay kit (A030-2-1; Nanjing Jiancheng Biotechnology).

Quantitative real-time PCR (qRT-PCR)

TransZol Up (ET111-01; Tansgen, Beijing, China) was utilized to isolate total RNA from liver tissues. The RNA level was assessed with a nucleic acid analyzer (BioPhotometer® D30; Eppendorf, Hamburg, Germany). A PrimeScriptTM RT Reagent Kit with gDNA Eraser (RR047A; Takara, Beijing, China) was used for reverse

transcription to synthesize stable cDNA, and TB Green® Premix Ex Taq $^{\rm TM}$ II (RR820A; Takara) was used to perform RT-qPCR. The RT-qPCR conditions were set at 95°C for 30 s, followed by 40 cycles of 95°C for 5 s and 60°C for 34 s, and a QuantStudio 3 PCR detection system from Thermo Fisher Scientific (Waltham, USA) was used. All primer sequences were designed and synthesized by Sangon Biotech (Shanghai, China), as listed in Table 1. The target mRNA levels were normalized to those of *GAPDH*, which served as the endogenous control. Each experiment was conducted in triplicate. The relative changes in mRNA expression were determined via the $2^{-\Delta\Delta Ct}$ method, which guarantees the amplification of a single product in each PCR analysis.

Histopathology

Fresh liver tissues were fixed in 4% paraformaldehyde for 24 h. Paraffin sections were prepared through dehydration, wax immersion, embedding, and sectioning. The 4-µm paraffin sections were then dewaxed and stained with hematoxylin and eosin (H&E) (G1120; Solarbio, Beijing, China), Masson (MST-8003; Maixin Biotech, Fuzhou, China), and Sirius red (G1472; Solarbio). After staining, the sections were dehydrated, sealed, and examined via a PA53 biological microscope (Motic, Xiamen, China). Images were captured and analyzed with Image J software.

Calculation of the residual liver regeneration rate

The resected liver masses of the animals were weighed after PH. The initial total liver weight was calculated via the following formula: (resected liver weight / 70) \times 100 (g). At the time of sacrifice, the animals and their regenerated liver masses were weighed. The percentage of liver reconstitution was calculated as (Regenerated liver weight / Initial total liver weight) \times 100%. The liver-to-body weight ratio was determined as follows: (Liver weight $_{\rm regenerated}$ / Body weight $_{\rm time\ of\ harvest}$) \times 100%.

Immunohistochemical staining

The paraffin sections were processed by dewaxing and rehydration. First, liver tissue slices were heat-fixed at $60\,^{\circ}\text{C}$ for 30 min, followed by deparaffinization in xylene for 20 min, rehydration in a series of ethanol concentrations ($100\,\%$, $95\,\%$, $85\,\%$, and $75\,\%$) for 5 min each, and then rinsing thrice with PBS at room temperature for 5 min per wash. Antigen retrieval was performed using a Tris-EDTA solution (pH 9.0) (P0084; Beyotime Biotechnology, Shanghai, China) in a microwave oven at $100\,^{\circ}\text{C}$ for 15 min. Endogenous peroxidase activity was blocked by incubating the sections in $3\,\%$ H_2O_2 for 10 min in the dark. Following overnight incubation at $4\,^{\circ}\text{C}$,

the sections were incubated with the following primary antibodies: alpha smooth muscle actin (α-SMA), Ki67, and PCNA (14395-1-AP, 27309-1-AP, 24036-1-AP; Proteintech Corporation, Chicago, USA). The sections were subsequently washed three times with PBS at room temperature for 5 min each. Next, an HRP-conjugated secondary antibody (PV-6000; ZSGB-BIO, Beijing, China) was applied, and the samples were incubated at 37°C for 20 min, followed by three times wash with PBS. The reaction products were visualized with 3,3′-diaminobenzidine (DAB) (ZLI-9017; ZSGB-BIO) and counterstained with hematoxylin. The slices were dehydrated by immersion in 75%, 85%, 95%, and 100% ethanol, followed by xylene for 5 min each. Positive cells were observed and imaged via the PA53 biological microscope. Identification and quantification were performed via ImageJ software [32].

Western blot analysis

The lysis buffer consisted of PMSF (AR1178; Boster, Wuhan, China) and RIPA lysis buffer (PC101; Epizyme Biotech, Shanghai, China) at a 1:100 ratio. Liver tissue was dissolved in lysis buffer at 4°C for 30 min, and the lysates were subsequently centrifuged at 10,000 g for 15 min at 4°C. The supernatant was collected for further analysis. Protein concentrations were measured via a BCA protein assay kit (ZJ102; Epizyme Biotech) and equalized via the addition of lysis buffer. The protein buffer and sample protein were subsequently combined at a 1:4 ratio and heated at 100°C for 10 min to denature the proteins. Equal quantities of protein samples were separated via a 10% SDS-PAGE and subsequently transferred onto a PVDF membrane in an ice bath. The membranes were blocked with 5% skim milk in Tris-buffered saline with 0.1% Tween-20 (TBST) for 2 h at room temperature and washed three times with TBST. The membranes were incubated overnight at 4°C with primary antibodies against Wnt3a, β-catenin, cyclin D1, c-Myc (WL02179, WL0962a, WL01435a, WL01781; Wanleibio, Shenyang, China), α-SMA, PCNA and GAPDH (14395-1-AP, 24036-1-AP, 60004-1-Ig; Proteintech Corporation). The PVDF membrane was subsequently washed three times with TBST before being incubated with secondary antibodies (bs-0295G-HRP; Bioss, Beijing, China) at 4°C for 2 h. The target proteins were visualized via an enhanced chemiluminescence substrate kit (BMU102-CN; Abbkine, Wuhan, China), and the net optical density was analyzed via Image J software.

Statistics and analysis

The data were analyzed and plotted via Graph Pad Prism Version 9. All the results are expressed as the mean \pm SD. Statistical

Table 1. Sequences of primers used in RT-qPCR

Gene	Forward primer (5′→3′)	Reverse primer (5'→3')
IL-1	CCACCTTTTGACAGTGATGA	GAGATTTGAAGCTGGATGCT
IL-6	GTCGGAGGCTTAATTACACA	TTTTCTGCAAGTGCATCATC
IL-10	GGTTGCCAAGCCTTATCGGAAATG	GCCGCATCCTGAGGGTCTTC
TNF-α	CCCTCCAGAAAAGACACCATG	GCCACAAGCAGGAATGAGAAG
HGF	AACAGGGGCTTTACGTTCACT	CGTCCCTTTATAGCTGCCTCC
EGF	TGGTCCTGCTCGTCTTGG	GTCCGCTGCTCACACTTC
VEGF	GTGACAAGCCAAGGCGGTGAG	CGATGATGGCGTGGTGAC
FGF	GATCATGCTTCCACCTCGTCTGTC	AGTTCACACTCGTAGCCGTTTGC
GAPDH	CCACTCACGGCAAATTCAAC	CTCCACGACATACTCAGCAC

significance was assessed through one-way ANOVA followed by Dunnett's post hoc test for multiple comparisons. Statistical differences were deemed significant at P < 0.05.

Results

Identification and characterization of H-uc MSCs

In order to investigate the therapeutic effect of H-uc MSCs on liver regeneration after PH in liver fibrosis, we first examined and identified the extracted H-uc MSCs. Under an optical microscope, the isolated H-uc MSCs exhibited adherent growth ability, uniform distribution, and a spindle-shaped appearance (Figure 1B). To identify the pluripotency of H-uc MSCs, differentiation into adipocytes and osteoblasts was induced via specific media. Oil Red O and Alizarin Red S staining demonstrated their differentiation potential, as evidenced by the formation of lipid droplets in adipocytes and red calcium salt deposition in osteoblasts (Figure 1C). Flow cytometry analysis revealed high expressions of phenotype markers in H-uc MSCs, with 99.6%, 99.9%, and

99.9% of cells positive for CD105, CD90, and CD73, respectively. Conversely, CD11b, CD19, CD45, CD34 and HLA-DR were expressed at low levels in H-uc MSCs (Figure 1B). These data indicate that the cells we extracted were H-uc MSCs.

H-uc MSCs treatment improves liver function and reduces liver inflammation

First, we observed the gross morphological changes of the liver to determine liver damage and recovery. The appearance of liver tissue in the control and Oil + PH groups was reddish-brown, soft, and smooth, with no fibrosis observed. In contrast, after 9 weeks of CCl₄ administration, the liver tissue in the CCl₄ + PH and CCl₄ + PH + MSC groups exhibited a lighter color, coarse texture, and granular sensation, with hard fibrous capsules on the surface (Figure 2A). Although MSC treatment did not completely reverse CCl₄-induced liver damage, a notable improvement in liver morphology was observed (Figure 2A).

H&E staining is essential for evaluating cell degeneration and

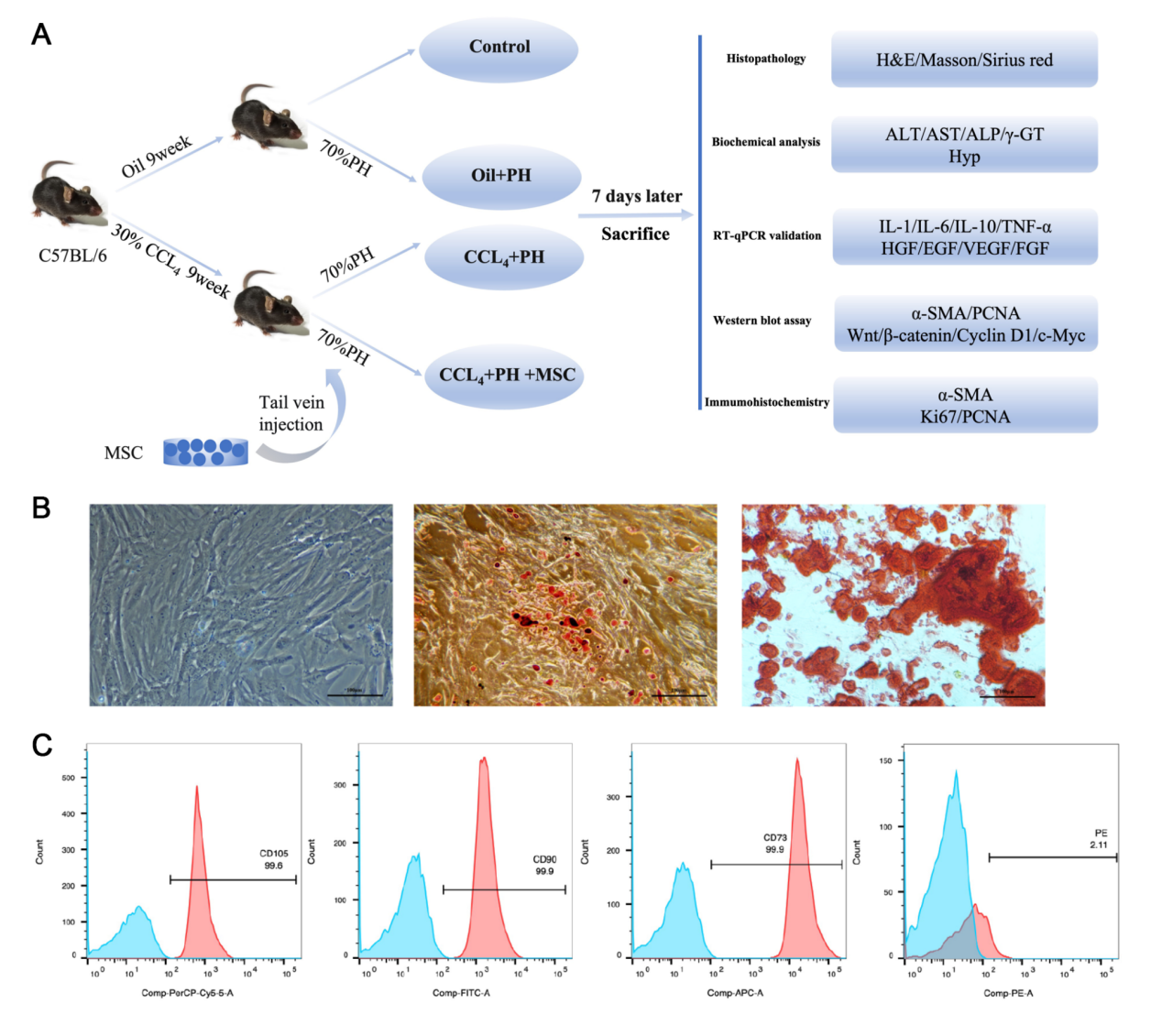


Figure 1. Characterization of H-uc MSCs (A) Study design. (B) Optical micrographs of the morphological characterization of MSCs at passage 4 (P4). Osteogenic differentiation of MSCs was assessed by alizarin red staining. Adipogenic differentiation of MSCs was assessed by Oil Red O staining. The magnification is 200× (scale bar: 100 µm). (C) Flow cytometry analysis of specific phenotype markers of MSCs at P4.

necrosis. In the control and Oil + PH groups, the structural integrity of the liver lobules was maintained, and the hepatocytes were arranged in hepatic lamellae with loosely distributed cytoplasm. In contrast, the CCl_4 + PH and CCl_4 + PH + MSC groups presented notable pathological changes, such as tissue necrosis, extensive inflammatory cell infiltration, hepatocyte degeneration, and fibrous hyperplasia around the veins. MSC treatment significantly improved liver pathology and alleviated liver injury (Figure 2B).

ALT, AST, ALP, and γ -GT levels are commonly used to assess liver function. The results revealed no significant changes in these

serum levels in the Oil + PH group compared with those in the control group. However, compared with those in the Oil + PH group, the ALT, AST, ALP, and γ -GT levels in the CCl₄ + PH group were significantly greater (Figure 2C–F, P < 0.05). After H-uc MSC treatment, the ALT, AST, ALP, and γ -GT levels in the CCl₄ + PH + MSC group were significantly lower than those in the CCl₄ + PH group (Figure 2C–F, P < 0.05). These findings suggest that H-uc MSC treatment improves liver function.

Additionally, inflammatory factor levels in liver tissue were assessed via qRT-PCR. Compared with the control group, the Oil +

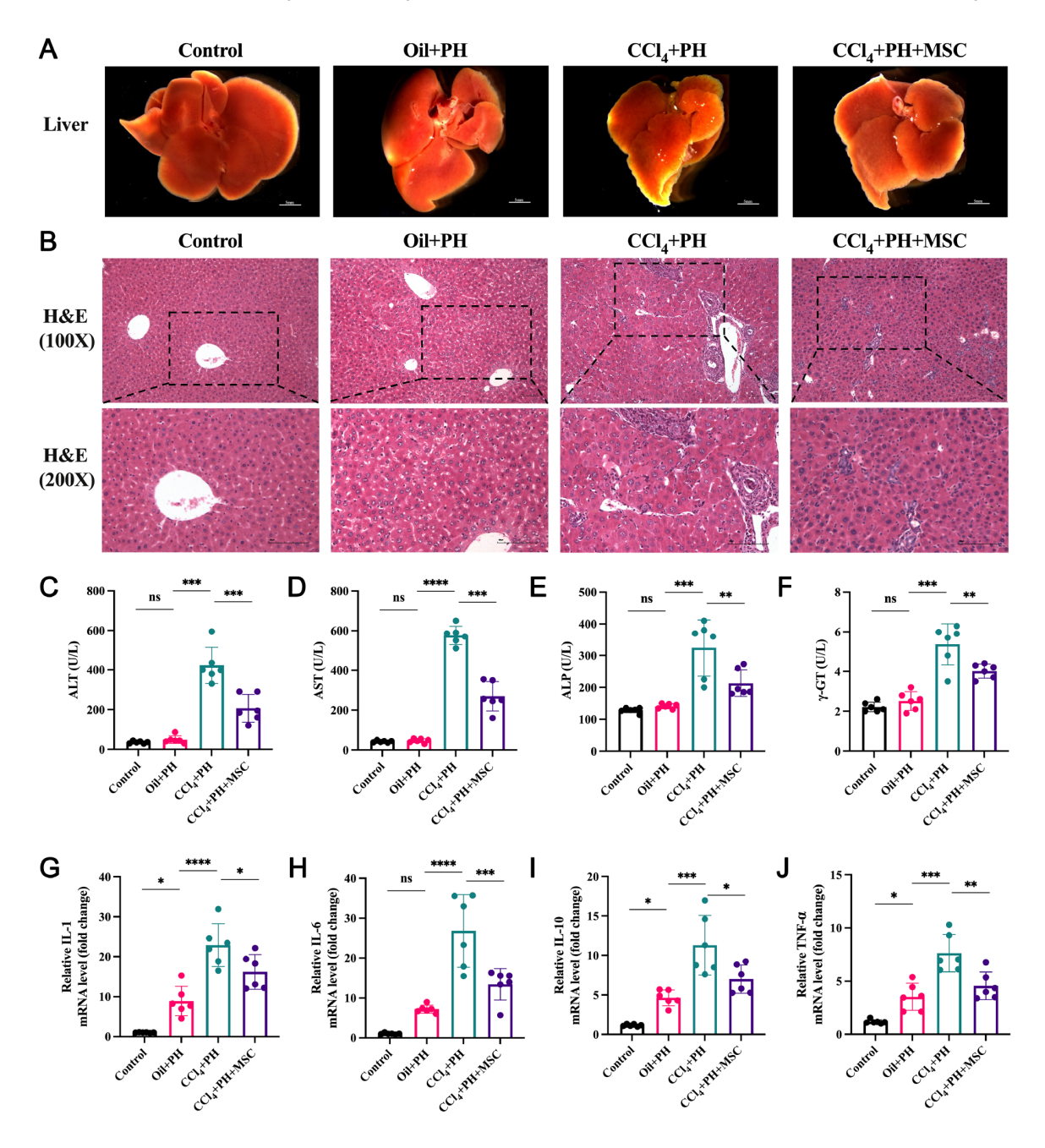


Figure 2. H-uc MSCs improve liver function and decrease inflammation (A) Representative images showing the gross liver morphology (scale bar: 5 mm). (B) Representative images of liver tissue sections subjected to H&E staining. The magnifications are 100× and 200× (scale bar: 100 μm). (C–F) Serum enzyme activities of ALT, AST, ALP and γ-GT. (G–J) Relative inflammatory gene expressions of *IL-1*, *IL-6*, *IL-10*, and *TNF-α*. Data are presented as the mean \pm SD, n = 6. *P < 0.05, **P < 0.01, ***P < 0.001, ****P < 0.0001.

PH group presented significantly increased IL-1, IL-6, IL-10, and TNF- α levels (Figure 2G–J, P < 0.05). The CCl₄ + PH group presented even greater increases in these inflammatory factors (Figure 2G–J, P < 0.05). Compared with the untreated CCl₄ + PH group, the CCl₄ + PH + MSC group presented significantly decreased expressions of IL-1, IL-6, IL-10, and TNF- α (Figure 2G–J, P < 0.05).

These results indicate that H-uc MSC treatment has an antifibrotic effect, as evidenced by improved liver function and reduced liver inflammation.

H-uc MSC treatment promotes hepatocyte regeneration

To investigate the potential of H-uc MSC treatment to promote hepatocyte proliferation, Ki67 and PCNA expression levels were analyzed through immunohistochemistry. Ki67 staining revealed lower expression in the control group than in the Oil + PH group and lower expression in the CCl_4 + PH group than in the Oil + PH group. In the fibrotic liver of the H-uc MSC-treated group, there was an increase in Ki67-positive cells compared with those in the untreated group exposed to CCl_4 + PH (Figure 3A,C, P < 0.05). Comparable findings were obtained by IHC of PCNA (Figure 3B,D).

Figure 3E shows the liver regeneration rates in the four groups of mice, expressed as a percentage of liver mass regeneration. At 7 days after PH, the liver mass regeneration rate was greater in the Oil + PH group than in the control group. In contrast, the CCl_4 + PH group presented a significantly lower regeneration rate than the Oil + PH group (P < 0.05). Interestingly, MSC treatment improved the liver regeneration rate, although it did not match the level observed in the Oil + PH group. Liver regeneration in the four groups of mice was assessed via the liver weight/body weight ratio (Figure 3F).

The PCNA protein in the livers of each group was subsequently detected via western blot analysis (Figure 3G). The findings revealed that the protein level of PCNA was lower in the control group than in the Oil + PH group and was also lower in the CCl₄ + PH group than in the Oil + PH group. However, after MSC treatment, the PCNA protein level in the CCl₄ + PH + MSC group was significantly greater than that in the CCl₄ + PH group (Figure 3H, P < 0.05). These findings were consistent with the IHC results. Overall, the proliferative capacity of fibrotic livers after PH was lower than that of normal livers after PH but significantly improved after MSC injection.

Additionally, compared with the control group, the Oil + PH group presented significantly increased expressions of the growth factors HGF and FGF, with no significant changes in EGF and VEGF levels (Figure 3I–L). Compared with the CCl_4 + PH group, the Oil + PH group presented significantly greater expressions of VEGF and FGF, with no changes in HGF and EGF levels (Figure 3I–L). Compared with the untreated CCl_4 + PH group, the CCl_4 + PH + MSC group presented significantly increased expressions of HGF, VEGF, and FGF (Figure 3I–L). These results indicate that MSCs can promote liver regeneration by increasing the secretion of growth factors.

H-uc MSC treatment can reduce the degree of liver fibrosis and inhibit the deposition of collagen

Given that collagen deposition is a key feature of liver fibrosis, histopathological staining was conducted to assess its distribution. Consistent with expectations, both Masson and Sirius Red staining revealed minimal collagen deposition in the control and Oil + PH groups. In contrast, extensive collagen fibers were observed in the

CCl₄ + PH and CCl₄ + PH + MSC groups. However, MSC treatment significantly reduced collagen fiber generation (Figure 4A,B,D,E).

The expression of α -SMA was evaluated through immunohistochemical staining, where α -SMA appeared yellow-brown in the liver tissue (Figure 4C). Compared with that in the control group, the percentage of α -SMA-positive cells in the Oil + PH group did not differ. The CCl₄ + PH group presented an increased positive rate of α -SMA, but the CCl₄ + PH + MSC group presented a reduced positive rate and histochemical scores of α -SMA (Figure 4F). Western blot analysis further confirmed that MSC treatment inhibited α -SMA expression at the protein level, which was consistent with the immunohistochemical results (Figure 4G,H). These findings demonstrate that MSCs can reduce liver fibrosis and attenuate collagen production.

Finally, fibrosis index measurements revealed a significant increase in HYP content in the CCl_4 + PH group, whereas the CCl_4 + PH + MSC group presented a marked decrease (Figure 4I).

H-uc MSC treatment promotes hepatocyte proliferation and liver regeneration by activating Wnt/ β -catenin signaling

Wnt/β-catenin signaling plays important roles in liver development, growth, metabolism and regeneration. To explore the relationship between H-uc MSC treatment and Wnt/β-catenin signaling in liver fibrosis, we analyzed Wnt/β-catenin-related protein levels in liver tissues via western blot analysis. Compared with that in the control group, liver regeneration in normal livers was greater after PH, which significantly promoted the expressions of Wnt3a, β-catenin, Cyclin D1, and c-Myc in liver tissues (Figure 5A–E). Compared with those in the Oil + PH group, the expressions of these proteins in the CCl₄ + PH group were significantly inhibited (Figure 5A–E). However, the administration of MSCs led to significant upregulation of Wnt3a, β-catenin, Cyclin D1, and c-Myc expressions in the CCl₄ + PH + MSC group compared with those in the CCl₄ + PH group (Figure 5A-E). These findings suggest that MSC therapy promotes hepatocyte proliferation and liver regeneration through the activation of Wnt/β-catenin signaling.

Discussion

MSCs have the ability to self-renew and undergo multidirectional differentiation, making them ideal cells for tissue regeneration and repair. Bone marrow, the umbilical cord, and adipose tissue are the most commonly used sources for obtaining MSCs. Studies have shown that MSCs from these sources not only have similar morphological characteristics and phenotypes but also possess the potential to differentiate into functional hepatocytes.

H-uc MSCs are easily obtained from umbilical cord tissue, cut and ligated after childbirth from healthy women. They primarily exist in Wharton's jelly and perivascular tissue of the umbilical cord and can be readily cultured and expanded *in vitro*. H-uc MSCs are "seed" cells capable of self-renewal and multilineage differentiation both *in vivo* and *in vitro*. Unlike invasive procedures such as bone marrow aspiration and liposuction, the collection of umbilical cord tissue is noninvasive and has no adverse effects on the mother or fetus. Additionally, since umbilical cord tissue is discarded after birth, its collection involves fewer ethical restrictions. These advantages make H-uc MSCs strong candidates for diverse clinical applications [33]. Since 2002, MSCs have been recognized for their strong immunosuppressive capabilities [34,35]. Later, Professor Le

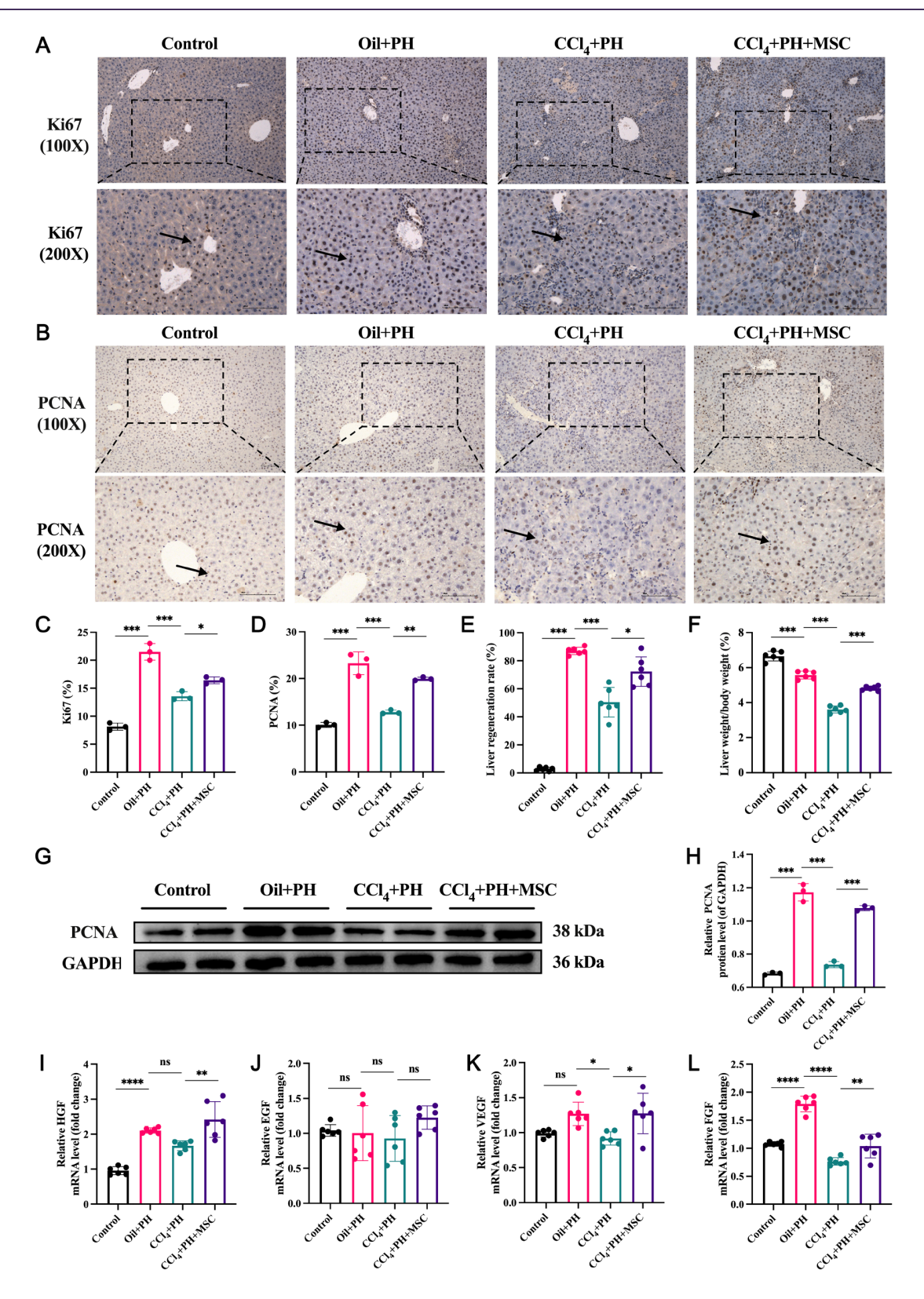


Figure 3. H-uc MSC treatment promotes liver regeneration (A) Photomicrographs of liver tissue sections showing IHC staining for Ki67 (black arrows indicate brown-positive cells). (B) Photomicrographs of liver tissue sections showing IHC staining for PCNA (black arrows indicate brown-positive cells). (C) Quantification of Ki67-positive cells. (D) Quantification of PCNA-positive cells. (E) Liver regeneration rates in the four groups of mice. (F) Liver weight/body weight ratio. (G) Western blot analysis of the PCNA protein. (H) Quantification of the relative intensity of PCNA protein. (I–L) The relative growth factor gene expressions of *HGF*, *EGF*, *VEGF*, and *FGF*. Data are presented as the mean \pm SD, n = 6. *P < 0.05, **P < 0.01, ****P < 0.001. Scale bar: 100 μ m.

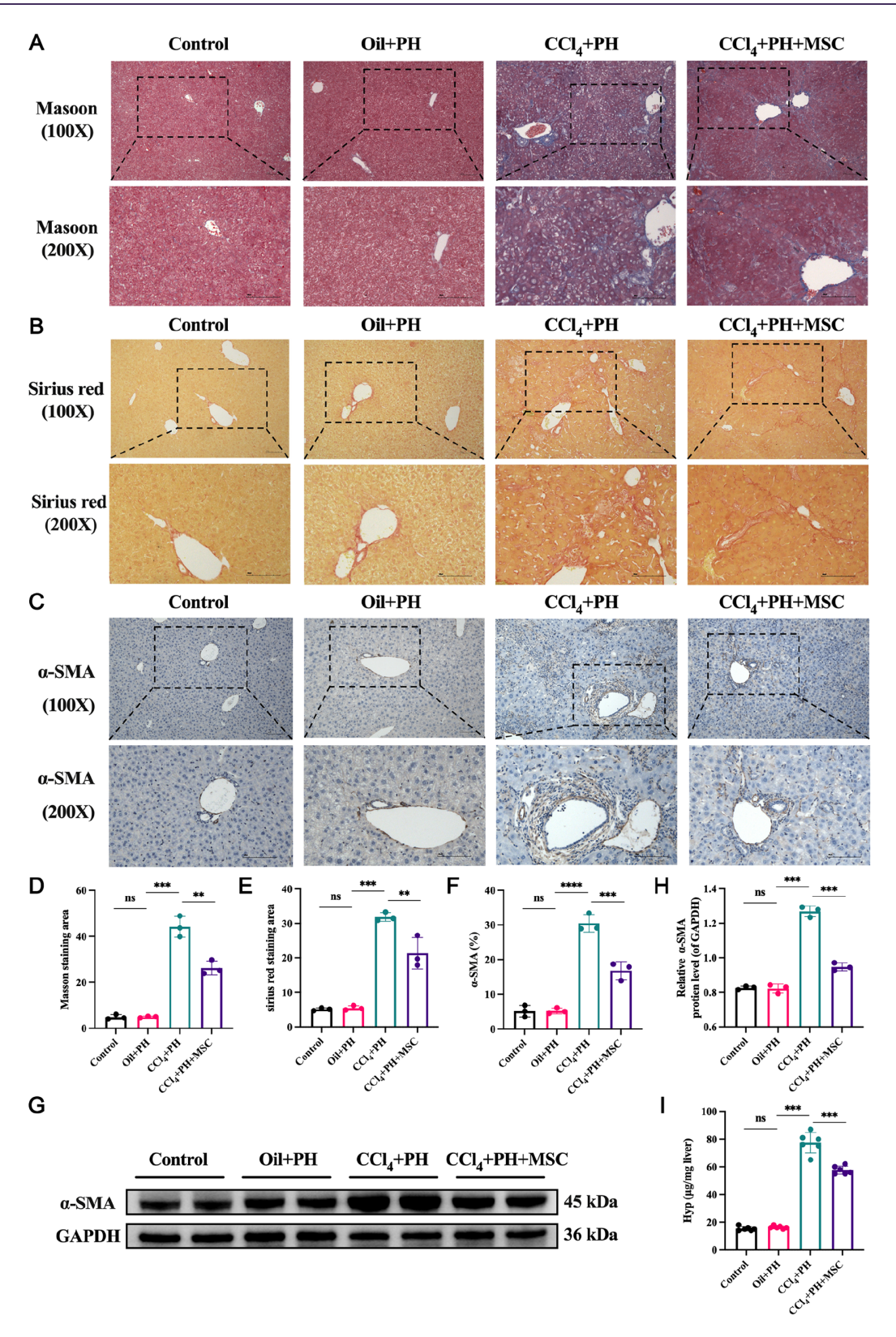


Figure 4. H-uc MSCs alleviate liver fibrosis in mice (A) Representative images of liver tissue sections subjected to Masson staining. The magnifications are $100 \times$ and $200 \times$. (B) Representative images of liver tissue sections subjected to Sirius red staining. The magnifications are $100 \times$ and $200 \times$. (C) Photomicrographs of liver tissue sections showing IHC staining for α -SMA. The magnifications are $100 \times$ and $200 \times$. (D) Quantitative results of Masson staining. (E) Quantitative results of Sirius red staining. (F) Quantification of α -SMA-positive cells. (G) Western blot analysis of the α -SMA protein. (H) Quantification of the relative α -SMA protein intensity. (I) Quantitative analysis of hepatic Hyp content. Data are presented as the mean \pm SD, n = 6. *P < 0.05, **P < 0.01, ****P < 0.001, ***

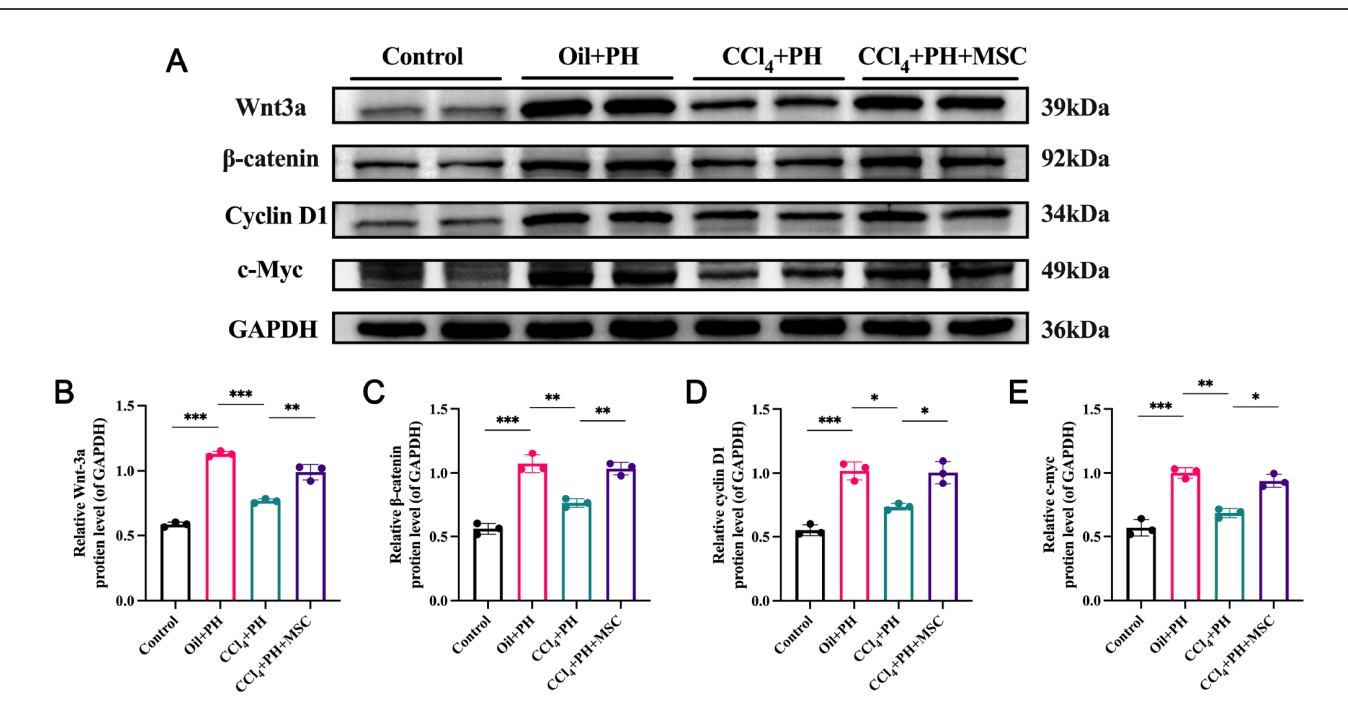


Figure 5. H-uc MSCs activate Wnt/β-catenin signaling (A) Representative western blots of Wnt3a, β-catenin, Cyclin D1, and c-Myc in liver tissue. (B) Quantification of the relative intensity of the Wnt3a protein. (C) Quantification of the relative β-catenin protein intensity. (D) Quantification of the relative intensity of the Cyclin D1 protein. (E) Quantification of the relative intensity of the c-Myc protein. Data are presented as the mean \pm SD, n = 6. *P < 0.05, *P < 0.01, **P < 0.01.

Blanc's team reported that MSCs have low immunogenicity and do not cause immune rejection even when they are used heterologously or across species [36]. Moreover, studies have shown that MSCs, regardless of their source (bone marrow, fat, placenta, etc.), express Class I leukocyte antigen (HLA)-ABC but not Class II histocompatibility molecules (HLA-DR) or costimulatory molecules such as CD40, CD80, and CD86, indicating their low immunogenicity. Compared with other MSCs, H-uc MSCs exhibit greater proliferative potential and lower allogeneic immunogenicity. Their therapeutic effects include cell replacement and strong paracrine actions, making them suitable for allogeneic or interallogeneic transplantation to treat tissue injuries and ischemic hypoxic diseases. Therefore, H-uc MSCs hold significant promise for broad clinical applications [37–39].

The liver possesses a unique and powerful regenerative ability, making it the organ with the strongest regenerative capacity. Understanding liver regeneration is crucial for improving outcomes in common liver surgeries and accelerating the recovery of liver function after transplantation [40,41]. Liver regeneration is a multifaceted process that involves various liver cell types, such as hepatocytes, hepatic stellate cells, endothelial cells, and inflammatory cells [42]. Hepatocytes are the main parenchymal cells and account for most liver functions [43]. In a healthy liver, hepatocyte mitosis is generally static. However, following toxic injury or partial hepatectomy, the number of liver cells is significantly reduced. Feedback signals stimulate hepatocyte proliferation, allowing cells to rapidly enter the cell cycle and restore liver mass and function. Liver regeneration involves the regeneration of parenchymal cells and the reconstruction of liver tissue structure. Various cytokines and growth factors regulate this process through different mechanisms. Liver regeneration depends on the balance between cell death and

proliferation, with cell death occurring through necrosis or apoptosis. During regeneration, parenchymal and nonparenchymal cells interact closely to promote the repair of liver mass and function [42,44].

The mechanism of liver regeneration is complicated. Hu et al. [45] reported that MSCs can promote liver regeneration by regulating immune cells. Song et al. [46] discovered that HUCB-MSC-derived exosomal miR-124 could enhance rat liver regeneration after PH by downregulating Foxg1. Xu et al. [47] demonstrated that exosomal miR-182-5p from hypoxic bone marrow mesenchymal stromal cells promotes liver regeneration via FOXO1-mediated macrophage polarization. Additionally, peroxisome proliferatoractivated receptor- α has been reported to regulate liver regeneration through the Yes-associated protein (YAP)-TEA domain transcription factor (TEAD) pathway [48]. These results indicate that MSCs have a notable effect on liver regeneration. Immunohistochemical staining and western blot analysis were utilized to quantify alterations in the proliferation-related proteins Ki67 and PCNA across each group of mice. The results demonstrated that the proliferative ability of the liver in the CCl₄ + PH group decreased after PH compared with that in the Oil + PH group. However, the proliferative ability of fibrotic livers in the CCl₄ + PH + MSC group significantly improved after MSC injection.

Liver tissue has a strong regenerative capacity, and calculating the residual liver weight regeneration rate can effectively reflect this process because of its simplicity and speed. A significant portion of the liver was removed in this experiment, leaving a small volume of remaining liver. Consequently, the compensatory mechanism was activated, leading to increased hepatocyte proliferation and enhanced liver tissue regeneration. By the 7th day after surgery, the liver regeneration rate in the Oil + PH group had approached 100%, demonstrating the robust regenerative ability of the liver

after surgery and trauma. Despite not reaching normal level, the liver regeneration rate in the $CCl_4 + PH + MSC$ group was notably elevated compared with that in the $CCl_4 + PH$ group.

Recent evidence suggests that the biotherapeutic effects of MSCs are largely due to bioactive factors produced through their paracrine mechanisms, which act on recipient cells to elicit biological effects. H-uc MSCs can secrete numerous molecular substances and cytokines with biological functions, effectively promoting damage repair, vascular regeneration, and blood circulation reconstruction [49,50]. Our experimental results revealed that the expressions of growth factors such as HGF and FGF were greater in the Oil + PH group than in the control group. Compared with those in the CCl₄ + PH + MSC group were significantly greater. Interestingly, there was no significant alteration in EGF mRNA levels, indicating that H-uc MSCs may promote liver regeneration by promoting the secretion of HGF and other growth factors. These results indicate that H-uc MSCs can improve the regeneration of liver tissue after PH in mice.

Although numerous studies have examined the involvement of various growth factors [51], cytokines [52], miRNAs [53] and long noncoding RNAs (lncRNAs) [54] in regulating gene expression and promoting liver regeneration, these studies have primarily used normal PH models. Further research is needed to investigate the factors involved in regulating liver regeneration after PH in liver fibrosis.

HSCs are a small cell population in the liver that play important roles in the occurrence and development of liver fibrosis and the initiation and termination of liver regeneration after liver injury [55-58]. Studies have shown that H-uc MSCs inhibit the activation of HSCs through the miR-148a-5p/SLIT3 pathway, thereby alleviating liver fibrosis [59]. However, tonsillar-derived MSC-EVs can reduce HSC activation and liver fibrosis through miR-486-5p [60]. Similar studies have also shown that MSC-EVs can inhibit the activation of HSCs in liver fibrosis through the miR-141-3p/PTEN/protein kinase B (Akt) pathway, thereby alleviating liver fibrosis [61]. These studies indicated that HSCs are essential in liver fibrosis and regeneration. Masson and Sirius Red staining revealed severe fibrosis in the CCl₄ + PH group compared with the Oil + PH group, whereas fibrosis was significantly reduced after H-uc MSC injection. Immunohistochemical staining and western blot analysis were utilized to assess changes in the expression of the fibrosis-related protein α -SMA. The results revealed decreased α -SMA expression in the CCl₄ + PH + MSC group, indicating reduced liver fibrosis after MSC treatment.

Wnt/ β -catenin signaling is a crucial regulatory mechanism in liver growth and development and is highly conserved across biological evolution. Activation of this pathway involves diverse and intricate modes, including alterations in the expressions of both upstream and downstream components. For example, miRNAs can activate Wnt/ β -catenin signaling by regulating APC in the multiprotein complex [62], whereas lncRNA-LALR1 can activate the pathway by inhibiting the expression of the scaffold protein Axin1 [54]. Studies have shown that the activation or degradation of Dv12 regulates Wnt/ β -catenin signaling [63]. The activation of Wnt/ β -catenin signaling can promote liver regeneration in mice [64,65]. Therefore, we assessed the protein levels associated with Wnt/ β -catenin signaling in mouse liver tissues. The results showed that activating Wnt/ β -catenin signaling in the Oil + PH group after PH promoted liver regeneration. However, Wnt/ β -catenin signaling was inhibited

after PH in hepatic fibrosis.

The cyclin family has emerged as a prominent downstream target of Wnt/ β -catenin signaling. Activation of this pathway leads to the upregulation of Cyclin D1 expression. Previous studies have reported that Wnt/ β -catenin signaling can regulate hepatocyte growth by modulating the expressions of Cyclin family genes [54]. Increased Cyclin D1 expression is necessary for the transition from the G1 to S phase in hepatocyte proliferation. Our findings underscore the pivotal regulatory function of Wnt/ β -catenin signaling on the Cyclin family, which enhances Cyclin expression through nuclear translocation and promotes hepatocyte cycle progression and proliferation during liver regeneration. Additionally, the expressions of Wnt signaling proteins (Wnt3a and β -catenin) can be upregulated under MSC treatment, subsequently increasing the levels of downstream genes (Cyclin D1 and c-Myc).

Previous studies have suggested that Wnt/β-catenin signaling enhances cell growth and has anti-inflammatory and fibrosis inhibitory effects [66,67]. Therefore, we further analyzed the level of inflammation in cells after MSC treatment and detected a reduction in inflammation in the experimental group. In addition, α -SMA expression in liver tissue serves as an indicator of hepatic stellate cell activation, and its upregulation is associated with the occurrence and progression of liver fibrosis [68,69]. Our findings indicated that H-uc MSC treatment significantly reduced α-SMA expression in vivo. These results suggest that inflammation and collagen fiber level decreased in the CCl₄ + PH + MSC group, although the impact was not as remarkable as the increase in cell growth. Therefore, we concluded that liver regeneration is promoted primarily through direct activation of Wnt/β-catenin signaling, which enhances hepatocyte growth, whereas antiinflammatory effects are not the main effect.

In summary, after PH in mice, the liver has strong regenerative and repair ability, quickly restoring liver function to normal level. This study confirmed the activation of Wnt/ β -catenin signaling during hepatocyte proliferation, highlighting its crucial role in liver regeneration and repair. MSC treatment can promote liver regeneration and repair damaged liver cells by activating Wnt/ β -catenin signaling and alleviating liver fibrosis to some extent. However, the specific functions and mechanisms of this process require further study. This research provides a new target and theoretical basis for the recovery of liver function and prevention of liver failure in patients with clinical liver fibrosis after PH.

Funding

This work was supported by the grant from the Natural Science Foundation of Shanxi Province (No. 202103021223243).

Conflict of Interest

The authors declare that they have no conflict of interest.

References

- Ohtani N, Kawada N. Role of the gut-liver axis in liver inflammation, fibrosis, and cancer: a special focus on the gut microbiota relationship. Hepatol Commun 2019, 3: 456–470
- Tateishi R, Uchino K, Fujiwara N, Takehara T, Okanoue T, Seike M, Yoshiji H, et al. A nationwide survey on non-B, non-C hepatocellular carcinoma in Japan: 2011–2015 update. J Gastroenterol 2019, 54: 367–376
- 3. Kisseleva T, Brenner DA. Mechanisms of fibrogenesis. *Exp Biol Med (Maywood)* 2008, 233: 109–122

- Sun M, Kisseleva T. Reversibility of liver fibrosis. Clin Res Hepatol Gastroenterol 2015, 39: S60–S63
- Kisseleva T, Brenner D. Molecular and cellular mechanisms of liver fibrosis and its regression. Nat Rev Gastroenterol Hepatol 2021, 18: 151– 166
- Venturi C, Sempoux C, Quinones JA, Bourdeaux C, Hoyos SP, Sokal E, Reding R. Dynamics of allograft fibrosis in pediatric liver transplantation. *Am J Transplant* 2014, 14: 1648–1656
- Fausto N. Liver regeneration: from laboratory to clinic. Liver Transplant 2001. 7: 835–844
- Shiffman M, Brown RS, Olthoff KM, Everson G, Miller C, Siegler M, Hoofnagle JH. Living donor liver transplantation: summary of a conference at The National Institutes of Health. *Liver Transplant* 2002, 8: 174–188
- Schindl MJ, Redhead DN, Fearon KC, Garden OJ, Wigmore SJ. The value of residual liver volume as a predictor of hepatic dysfunction and infection after major liver resection. *Gut* 2005, 54: 289–296
- Kwon YJ, Lee KG, Choi D. Clinical implications of advances in liver regeneration. Clin Mol Hepatol 2015, 21: 7–13
- Riehle KJ, Dan YY, Campbell JS, Fausto N. New concepts in liver regeneration. J Gastro Hepatol 2011, 26: 203–212
- Seki T, Yokoyama Y, Nagasaki H, Kokuryo T, Nagino M. Adipose tissuederived mesenchymal stem cell transplantation promotes hepatic regeneration after hepatic ischemia-reperfusion and subsequent hepatectomy in rats. *J Surg Res* 2012, 178: 63–70
- Kaibori M, Adachi Y, Shimo T, Ishizaki M, Matsui K, Tanaka Y, Ohishi M, et al. Stimulation of liver regeneration after hepatectomy in mice by injection of bone marrow mesenchymal stem cells via the portal vein. Transplant Proc 2012, 44: 1107–1109
- 14. Yu J, Yin S, Zhang W, Gao F, Liu Y, Chen Z, Zhang M, et al. Hypoxia preconditioned bone marrow mesenchymal stem cells promote liver regeneration in a rat massive hepatectomy model. Stem Cell Res Ther 2013, 4: 83
- Li DL, He XH, Zhang SA, Fang J, Chen FS, Fan JJ. Bone marrow-derived mesenchymal stem cells promote hepatic regeneration after partial hepatectomy in rats. *Pathobiology* 2013, 80: 228–234
- Eom YW, Shim KY, Baik SK. Mesenchymal stem cell therapy for liver fibrosis. Korean J Intern Med 2015, 30: 580–589
- Liu WH, Song FQ, Ren LN, Guo WQ, Wang T, Feng YX, Tang LJ, et al. The multiple functional roles of mesenchymal stem cells in participating in treating liver diseases. J Cell Mol Medi 2015, 19: 511–520
- 18. Alfaifi M, Eom YW, Newsome PN, Baik SK. Mesenchymal stromal cell therapy for liver diseases. *J Hepatol* 2018, 68: 1272–1285
- 19. Meier RPH, Mahou R, Morel P, Meyer J, Montanari E, Muller YD, Christofilopoulos P, *et al.* Microencapsulated human mesenchymal stem cells decrease liver fibrosis in mice. *J Hepatol* 2015, 62: 634–641
- 20. Rengasamy M, Singh G, Fakharuzi NA, Siddikuzzaman NA, Balasubramanian S, Swamynathan P, Thej C, *et al.* Transplantation of human bone marrow mesenchymal stromal cells reduces liver fibrosis more effectively than Wharton's jelly mesenchymal stromal cells. *Stem Cell Res Ther* 2017, 8: 143
- Chai NL, Zhang XB, Chen SW, Fan KX, Linghu EQ. Umbilical cord-derived mesenchymal stem cells alleviate liver fibrosis in rats. World J Gastroenterol 2016, 22: 6036–6048
- Yin K, Wang S, Zhao RC. Exosomes from mesenchymal stem/stromal cells: a new therapeutic paradigm. *Biomark Res* 2019, 7: 8
- 23. He S, Tang S. WNT/β-catenin signaling in the development of liver cancers. *Biomed Pharmacother* 2020, 132: 110851
- 24. Perugorria MJ, Olaizola P, Labiano I, Esparza-Baquer A, Marzioni M,

- Marin JJG, Bujanda L, *et al.* Wnt-β-catenin signalling in liver development, health and disease. *Nat Rev Gastroenterol Hepatol* 2019, 16: 121–
- Annunziato S, Sun T, Tchorz JS. The RSPO-LGR4/5-ZNRF3/RNF43 module in liver homeostasis, regeneration, and disease. *Hepatology* 2022, 76: 888–899
- Fu YS, Cheng YC, Lin MYA, Cheng H, Chu PM, Chou SC, Shih YH, et al. Conversion of human umbilical cord mesenchymal stem cells in wharton' s jelly to dopaminergic neurons in vitro: potential therapeutic application for parkinsonism. Stem Cells 2006, 24: 115–124
- Mitchell C, Willenbring H. A reproducible and well-tolerated method for 2/3 partial hepatectomy in mice. *Nat Protoc* 2008, 3: 1167–1170
- Dong S, Chen QL, Song YN, Sun Y, Wei B, Li XY, Hu YY, et al. Mechanisms of CCl₄-induced liver fibrosis with combined transcriptomic and proteomic analysis. J Toxicol Sci 2016, 41: 561–572
- Shrestha N, Chand L, Han MK, Lee SO, Kim CY, Jeong YJ. Glutamine inhibits CCl4 induced liver fibrosis in mice and TGF-β1 mediated epithelial–mesenchymal transition in mouse hepatocytes. *Food Chem Toxicol* 2016, 93: 129–137
- Yagi S, Hirata M, Miyachi Y, Uemoto S. Liver regeneration after hepatectomy and partial liver transplantation. *Int J Mol Sci* 2020, 21: 8414
- Lee J, Garcia V, Nambiar SM, Jiang H, Dai G. Pregnancy facilitates maternal liver regeneration after partial hepatectomy. Am J Physiol Gastrointestinal Liver Physiol 2020, 318: G772–G780
- Varghese F, Bukhari AB, Malhotra R, De A, Aziz SA. IHC profiler: an open source plugin for the quantitative evaluation and automated scoring of immunohistochemistry images of human tissue samples. *PLoS One* 2014, 9: e96801
- Nagamura-Inoue T. Umbilical cord-derived mesenchymal stem cells: their advantages and potential clinical utility. WJSC 2014, 6: 195–202
- 34. Bartholomew A, Sturgeon C, Siatskas M, Ferrer K, McIntosh K, Patil S, Hardy W, *et al.* Mesenchymal stem cells suppress lymphocyte proliferation *in vitro* and prolong skin graft survival *in vivo*. *Exp Hematol* 2002, 30: 42–48
- Di Nicola M, Carlo-Stella C, Magni M, Milanesi M, Longoni PD, Matteucci P, Grisanti S, et al. Human bone marrow stromal cells suppress Tlymphocyte proliferation induced by cellular or nonspecific mitogenic stimuli. Blood 2002, 99: 3838–3843
- 36. Le Blanc K. Immunomodulatory effects of fetal and adult mesenchymal stem cells. *Cytotherapy* 2003, 5: 485–489
- 37. Lee RH, Pulin AA, Seo MJ, Kota DJ, Ylostalo J, Larson BL, Semprun-Prieto L, et al. Intravenous hMSCs improve myocardial infarction in mice because cells embolized in lung are activated to secrete the anti-inflammatory protein TSG-6. Cell Stem Cell 2009, 5: 54–63
- He H, Zhao ZH, Han FS, Liu XH, Wang R, Zeng YJ. Overexpression of protein kinase C ε improves retention and survival of transplanted mesenchymal stem cells in rat acute myocardial infarction. *Cell Death Dis* 2016. 7: e2056
- Pittenger MF, Mackay AM, Beck SC, Jaiswal RK, Douglas R, Mosca JD, Moorman MA, et al. Multilineage potential of adult human mesenchymal stem cells. Science 1999, 284: 143–147
- Michalopoulos GK, Bhushan B. Liver regeneration: biological and pathological mechanisms and implications. *Nat Rev Gastroenterol Hepatol* 2021. 18: 40–55
- 41. Mao SA, Glorioso JM, Nyberg SL. Liver regeneration. *Transl Res* 2014, 163: 352–362
- Campana L, Esser H, Huch M, Forbes S. Liver regeneration and inflammation: from fundamental science to clinical applications. *Nat Rev Mol Cell Biol* 2021, 22: 608–624
- 43. Trefts E, Gannon M, Wasserman DH. The liver. Curr Biol 2017, 27: R1147-

R1151

- De Rudder M, Dili A, Stärkel P, Leclercq IA. Critical role of LSEC in posthepatectomy liver regeneration and failure. *Int J Mol Sci* 2021, 22: 8053
- 45. Hu C, Wu Z, Li L. Mesenchymal stromal cells promote liver regeneration through regulation of immune cells. *Int J Biol Sci* 2020, 16: 893–903
- Song XJ, Zhang L, Li Q, Li Y, Ding FH, Li X. hUCB-MSC derived exosomal miR-124 promotes rat liver regeneration after partial hepatectomy via downregulating Foxg1. *Life Sci* 2021, 265: 118821
- Xu J, Chen P, Yu C, Shi Q, Wei S, Li Y, Qi H, et al. Hypoxic bone marrow mesenchymal stromal cells-derived exosomal miR-182-5p promotes liver regeneration via FOXO1-mediated macrophage polarization. FASEB J 2022, 36: e22553
- 48. Fan S, Gao Y, Qu A, Jiang Y, Li H, Xie G, Yao X, et al. YAP-TEAD mediates PPARα-induced hepatomegaly and liver regeneration in mice. Hepatology 2022, 75: 74–88
- Mareschi K, Biasin E, Piacibello W, Aglietta M, Madon E, Fagioli F. Isolation of human mesenchymal stem cells: bone marrow versus umbilical cord blood. *Haematologica* 2001, 86: 1099–1100
- Li JP, Wang DW, Song QH. Transplantation of erythropoietin genetransfected umbilical cord mesenchymal stem cells as a treatment for limb ischemia in rats. *Genet Mol Res* 2015, 14: 19005–19015
- Matsumoto K, Miyake Y, Umeda Y, Matsushita H, Matsuda H, Takaki A, Sadamori H, et al. Serial changes of serum growth factor levels and liver regeneration after partial hepatectomy in healthy humans. Int J Mol Sci 2013, 14: 20877–20889
- Tachibana S, Zhang X, Ito K, Ota Y, Cameron AM, Williams GM, Sun Z. Interleukin-6 is required for cell cycle arrest and activation of DNA repair enzymes after partial hepatectomy in mice. *Cell Biosci* 2014, 4: 6
- John K, Hadem J, Krech T, Wahl K, Manns MP, Dooley S, Batkai S, et al. MicroRNAs play a role in spontaneous recovery from acute liver failure. Hepatology 2014, 60: 1346–1355
- 54. Xu D, Yang F, Yuan J, Zhang L, Bi H, Zhou C, Liu F, *et al.* Long noncoding RNAs associated with liver regeneration 1 accelerates hepatocyte proliferation during liver regeneration by activating wnt/β-catenin signaling. *Hepatology* 2013, 58: 739–751
- 55. Kamm DR, McCommis KS. Hepatic stellate cells in physiology and pathology. *J Physiol* 2022, 600: 1825–1837
- 56. Siapati EK, Roubelakis MG, Vassilopoulos G. Liver regeneration by hematopoietic stem cells: have we reached the end of the road? *Cells* 2022, 11: 2312
- 57. Zhang W, Conway SJ, Liu Y, Snider P, Chen H, Gao H, Liu Y, et al.

- Heterogeneity of hepatic stellate cells in fibrogenesis of the liver: insights from single-cell transcriptomic analysis in liver injury. *Cells* 2021, 10: 2129
- Ge JY, Zheng YW, Tsuchida T, Furuya K, Isoda H, Taniguchi H, Ohkohchi N, et al. Hepatic stellate cells contribute to liver regeneration through galectins in hepatic stem cell niche. Stem Cell Res Ther 2020, 11: 425
- Yuan M, Yao L, Chen P, Wang Z, Liu P, Xiong Z, Hu X, et al. Human umbilical cord mesenchymal stem cells inhibit liver fibrosis via the microRNA-148a-5p/SLIT3 axis. Int Immunopharmacol 2023, 125: 111134
- 60. Kim J, Lee C, Shin Y, Wang S, Han J, Kim M, Kim JM, et al. sEVs from tonsil-derived mesenchymal stromal cells alleviate activation of hepatic stellate cells and liver fibrosis through miR-486-5p. Mol Ther 2021, 29: 1471–1486
- 61. Ma L, Wei J, Zeng Y, Liu J, Xiao E, Kang Y, Kang Y. Mesenchymal stem cell-originated exosomal circDIDO1 suppresses hepatic stellate cell activation by miR-141-3p/PTEN/AKT pathway in human liver fibrosis.

 Drug Deliver 2022, 29: 440–453
- 62. Park MG, Kim JS, Park SY, Lee SA, Kim HJ, Kim CS, Kim JS, et al. MicroRNA-27 promotes the differentiation of odontoblastic cell by targeting APC and activating Wnt/β-catenin signaling. Gene 2014, 538: 266–272
- Sharma J, Mulherkar S, Mukherjee D, Jana NR. Malin regulates wnt signaling pathway through degradation of dishevelled2. *J Biol Chem* 2012, 287: 6830–6839
- Huang R, Zhang X, Gracia-Sancho J, Xie WF. Liver regeneration: cellular origin and molecular mechanisms. *Liver Int* 2022, 42: 1486–1495
- 65. Jung YS, Stratton SA, Lee SH, Kim MJ, Jun S, Zhang J, Zheng B, et al. TMEM9-v-ATPase activates wnt/β-catenin signaling via APC lysosomal degradation for liver regeneration and tumorigenesis. Hepatology 2021, 73: 776–794
- Kuncewitch M, Yang WL, Molmenti E, Nicastro J, Coppa GF, Wang P. Wnt agonist attenuates liver injury and improves survival after hepatic ischemia/reperfusion. Shock 2013, 39: 3–10
- Apte U, Singh S, Zeng G, Cieply B, Virji MA, Wu T, Monga SPS. Betacatenin activation promotes liver regeneration after acetaminopheninduced injury. *Am J Pathol* 2009, 175: 1056–1065
- 68. Wang YP, He Q, Wu F, Zhu LL, Liu W, Zhang YN, He YW. Effects of Wnt3a on proliferation, activation and the expression of TGFb/Smad in rat hepatic stellate cells. *Zhonghua Gan Zang Bing Za Zhi* 2013, 21: 111–115
- 69. Majumdar A, Curley SA, Wu X, Brown P, Hwang JP, Shetty K, Yao ZX, $\it et$ $\it al.$ Hepatic stem cells and transforming growth factor $\it \beta$ in hepatocellular carcinoma. *Nat Rev Gastroenterol Hepatol* 2012, 9: 530–538